European Journal of Neuroscience, Vol. 7, pp. 1989–2004, 1995

Properties of unitary IPSPs evoked by anatomically identified basket cells in the rat hippocampus

E. H. Buhl, S. R. Cobb, K. Halasy[1] and P. Somogyi
MRC Anatomical Neuropharmacology Unit, Oxford University, Mansfield Road, Oxford OX1 3TH, UK
[1]Department of Zoology & Cell Biology, Jozsef Attila University, Szeged, Hungary

Keywords: GABA, inhibition, presynaptic, postsynaptic, interneuron

Abstract

Hippocampal pyramidal cells receive GABA-mediated synaptic input from several distinct interneurons. In order to define the effect of perisomatic synapses, intracellular recordings were made with biocytin-containing microelectrodes from synaptically connected inhibitory and pyramidal cell pairs in subfields CA1 and CA3 of the rat hippocampus. Subsequent physiological analysis was restricted to the category of cells, here referred to as *basket cells* (n = 14), which had an efferent synaptic target profile (n = 282 synaptic contacts) of predominantly somatic (48.2%) and proximal dendritic synapses (45.0%). Electron microscopic analysis revealed that in two instances identified postsynaptic pyramidal cells received a total of 10 and 12 labelled basket cell synapses respectively. At an average membrane potential of –57.8 ± 4.6 mV, unitary inhibitory postsynaptic potentials (IPSPs; n = 24) had a mean amplitude of 450 ± 238 μV, a 10–90% rise time of 4.6 ± 3.2 ms and, measured at half-amplitude, a mean duration of 31.6 ± 18.2 ms. In most instances (n = 19) the IPSP decay could be fitted with a single exponential with a mean time constant of 32.4 ± 18.0 ms. Unitary basket cell-evoked IPSPs fluctuated widely in amplitude, ranging from the level of detectability to >2 mV. The response reversal of IPSPs (n = 5) was extrapolated to be at –74.9 ± 6.0 mV. Averages of unitary IPSPs had a mean calculated conductance of 0.95 ± 0.29 nS, ranging from 0.52 to 1.16 nS. Unitary basket cell IPSPs (n = 3) increased in amplitude by 26.3 ± 19.9% following bath application of the $GABA_B$ receptor antagonist CGP 35845A (1–4 μM), whereas subsequent addition of the $GABA_A$ receptor antagonist bicuculline (10–13 μM) reduced the IPSP amplitude to 13.5 ± 3.1% of the control response. Rapid presynaptic trains of basket cell action potentials resulted in the summation of up to four postsynaptic responses (n = 5). However, any increase in the rate of tonic firing (2- to 10-fold) led to a >50% reduction of the postsynaptic response amplitude. At depolarized membrane potentials, averaged IPSPs could be followed by a distinct depolarizing overshoot or postinhibitory facilitation (n = 4). At firing threshold, pyramidal cells fired postinhibitory rebound-like action potentials, the latter in close temporal overlap with the depolarizing overshoot. In conclusion, hippocampal basket cells have been identified as one source of fast, $GABA_A$ receptor-evoked perisomatic inhibition. Unitary events are mediated by multiple synaptic release sites, thus providing an effective mechanism to avoid total transmission failures.

Introduction

Hippocampal interneurons were recognized early as the major source of locally generated inhibition which is exerted on excitatory principal cells (Andersen *et al.*, 1963, 1964a, b). Far from being homogeneous, these γ-aminobutyric acid (GABA) releasing local-circuit neurons show great diversity. They may differ with respect to their content of neuropeptides (Somogyi *et al.*, 1984; Kosaka *et al.*, 1985; Sloviter and Nilaver, 1987; Deller and Leranth, 1990), calcium binding proteins (Kosaka *et al.*, 1987; Nitsch *et al.*, 1990; Gulyas *et al.*, 1991; Miettinen *et al.*, 1992), expression of neurotransmitter receptors (Baude *et al.*, 1993; McBain and Dingledine, 1993; McBain *et al.*, 1994), their synaptic inputs (Gulyas *et al.*, 1990; Halasy *et al.*, 1992; Miettinen and Freund, 1992) and their synaptic target specificity (Somogyi *et al.*, 1983, 1985; Gulyas *et al.*, 1993b; Halasy and Somogyi, 1993; Han *et al.*, 1993; Buhl *et al.*, 1994b). Although evidently heterogeneous, inhibitory interneurons and their microcircuits are both stereotyped, as modular building blocks which are repeated many times over, and specific, being members of a given class which is highly distinct due to the defined synaptic input–output relationships of its members.

Although the connectional rules of inhibitory microcircuits are gradually emerging in parallel with the advent of sophisticated techniques, the functional role of specific GABAergic mechanisms is far from being understood. This may be exemplified by the discovery that GABAergic synapses innervating the axon initial segment and

Received 10 April 1995, revised and accepted 6 June 1995

Correspondence to: E. H. Buhl

the soma–proximal dendritic region of pyramidal cells originate largely from two distinct sources. *Axo-axonic cells* terminate almost exclusively on the axon initial segment of principal cells (Somogyi *et al.*, 1983; Somogyi *et al.*, 1985; Soriano and Frotscher, 1989; Soriano *et al.*, 1990; Buhl *et al.*, 1994b), whereas *basket cells* innervate cell bodies and proximal dendrites (Halasy and Somogyi, 1993; Buhl *et al.*, 1994a). Thus, there are at least two types of anatomically non-equivalent local-circuit neuron which may mediate perisomatic inhibition (Andersen *et al.*, 1963, 1964a, b).

A major step towards defining the roles of interneurons was made by employing double recording techniques to reveal the postsynaptic effect of a single inhibitory neuron on a monosynaptically coupled principal cell (Knowles and Schwartzkroin, 1981; Miles and Wong, 1984, 1987; Lacaille *et al.*, 1987; Lacaille and Schwartzkroin, 1988; Miles, 1990; Scharfman *et al.*, 1990). Several of these studies were targeted at GABAergic neurons in different hippocampal layers and it emerged that neurons in different hippocampal strata are presumably segregated into two major classes which differ with respect to their efferent postsynaptic response. A single presynaptic cell elicits either a fast $GABA_A$ receptor-mediated inhibitory postsynaptic potential (IPSP) or a slow-onset prolonged IPSP which may be due to the activation of $GABA_B$ receptors (Lacaille and Schwartzkroin, 1988; Miles, 1990). However, as each layer contains the cell bodies and terminals of several classes of local-circuit neurons, laminar differences alone are insufficient criteria to define the effect of any of them. As it is not possible to recognize different classes of GABAergic interneurons unambiguously on physiological grounds, intracellularly recorded neurons must be therefore identified anatomically to ascertain their identity on the basis of their efferent connections (Gulyas *et al.*, 1993b; Han *et al.*, 1993; Buhl *et al.*, 1994a, b). Moreover, the synaptic effect of different cell types is determined not only by the location, but also by the number of synaptic release sites. Thus the anatomical characterization of connections which mediate unitary interactions between synaptically coupled neuron pairs can reveal the role of structural differences which may shape postsynaptic responses (Korn *et al.*, 1982; Gulyas *et al.*, 1993a; Buhl *et al.*, 1994a). In the present study this approach has been adopted to define the postsynaptic effects and functional microcircuits of hippocampal basket cells. Preliminary results have been published elsewhere (Buhl *et al.*, 1994a).

Materials and methods

Slice preparation

Young adult female Wistar rats (>150 g) were deeply anaesthetized by an intramuscular injection of ketamine (100 mg/kg) and xylazine (10 mg/kg). After cessation of pain reflexes the animals were intracardially perfused with ~30 ml of chilled artificial cerebrospinal fluid (ACSF), their brains were quickly removed and immersed in a beaker with chilled ACSF. With the aid of a vibroslice (Campden Instruments, Loughborough, UK) 400 μm thick slices were cut in the horizontal plane. The hippocampi were dissected free and transferred to a recording chamber where they were maintained at 34–35°C on a nylon mesh at the interface between oxygenated ACSF and a humidified atmosphere saturated with 95% O_2/5% CO_2. The flow rate was adjusted to 1.5 ml/min and the slices were allowed to equilibrate for >1 h. The ACSF for electrophysiological recordings was composed of (in mM) 126 NaCl, 3.0 KCl, 1.25 NH_2PO_4, 24 Na HCO_3, 2.0 $MgSO_4$, 2.0 $CaCl_2$ and 10 glucose. During the initial stages of the experiments (perfusion, cutting, incubation) all NaCl (126 mM) was replaced by equimolar sucrose (256 mM), thus preventing passive chloride entry, which has been suggested to

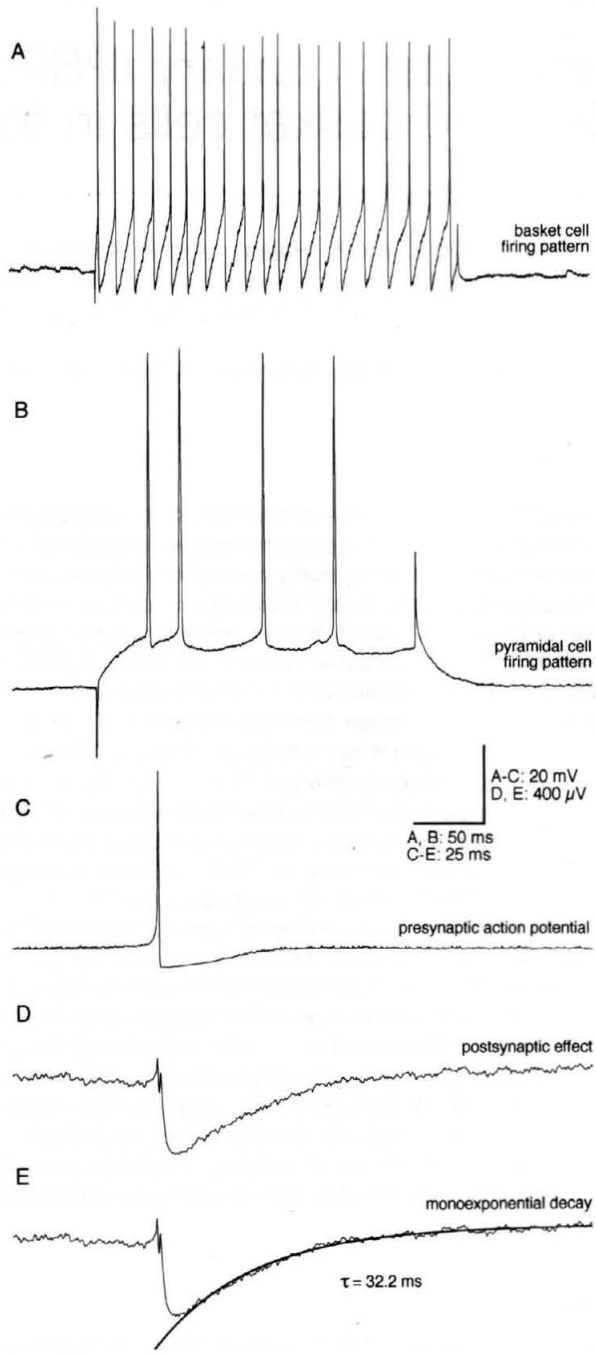

FIG. 1. Physiological identification of interneuron–pyramidal cell pairs. (A) During the experiments a search was made for cells which fired trains of non-accommodating action potentials and/or had short-duration action potentials which were followed by a deep fAHP. (B) While monitoring the impalement of the presumed interneuron shown in (A) a second microelectrode was advanced into cells that exhibited the physiological characteristics of pyramidal cells, such as marked spike frequency adaptation and relatively broad action potentials which were followed by a comparatively small fAHP. (C) Once two stable impalements had been achieved, the cell with interneuronal firing properties was depolarized by small increments of DC current until it fired. (D) Spike-triggered averaging techniques were then employed to determine whether both cells were synaptically coupled. If so, neurons with the properties shown in (A) invariably elicited short-latency IPSPs in the postsynaptic cells. (E) Unitary IPSPs were always of short duration and their decay phase could be frequently fitted with a single exponential function. Membrane potential in (D) = –62 mV. The traces in (D) and (E) represent an average of 135 sweeps. These two cells were identified anatomically using biocytin injections and are shown in Figure 2.

be acutely responsible for neurotoxicity during slice preparation (Aghajanian and Rasmussen, 1989). Usually the slices remained for 30 min in the sucrose solution before the perfusion medium was changed to normal ACSF. The drugs used in the pharmacology experiments were kept as concentrated stocks which were diluted in ACSF and then bath applied. The excitatory amino acid blockers 6-cyano-7-nitroquinoxaline-2,3-dione (CNQX) and DL-2-amino-5-phosphonopentanoic acid (AP5) were obtained from Tocris Cookson (Bristol, UK). Bicuculline hydrochloride was purchased from Sigma (Poole, UK) and the $GABA_B$ receptor antagonist CGP 55845A was made available by Drs Bittiger and Olpe (Ciba Geigy, Basle).

Intracellular recordings and data analysis

Recording electrodes were pulled from standard wall borosilicate tubing, filled with 2% biocytin (Horikawa and Armstrong, 1988) in 1.5 M KCH_3SO_4 and bevelled to a DC resistance of 80–150 MΩ. Recordings were obtained in the pyramidal cell layer of the CA1 and CA3 subfields. Putative interneurons were identified by their physiological characteristics, such as short-duration action potentials followed by large-amplitude fast afterhyperpolarizing potentials (fAHP; Fig. 1A). Once a stable recording had been obtained a search was made for cells displaying the electrophysiological properties of pyramidal neurons (Fig. 1B). Capacitive coupling was eliminated either off-line (Miles, 1990) or on-line using a modified Axoprobe (Axon Instruments, Foster City, CA) amplifier (Mason *et al.*, 1991). Synaptic coupling was tested using on-line spike-triggered averaging whilst eliciting firing in the interneuron with either depolarizing current pulses or constant DC current injections. Firing rates in the interneurons were adjusted by varying the current intensity and, depending on the particular protocol, ranged between 0.3 Hz and >100 Hz. Recordings were obtained with either an Axoclamp or Axoprobe amplifier (both Axon Instruments) which were operated in bridge mode. Experimental data were acquired using a PCM instrumentation recorder and stored on videotapes. Data analysis was continued off-line by (re)digitizing the data at 5–20 kHz using commercially available 12 Bit A/D boards (RC Electronics Computerscope, USA and National Instruments Labmaster$^+$, UK) in conjunction with Axograph (Axon Instruments), RC Electronics Computerscope (RC Electronics) and WCP (courtesy of Dr J. Dempster, University of Strathclyde, Glasgow, UK) software packages. Unless indicated otherwise data are expressed as mean ± SD.

Resting membrane potentials were determined following electrode withdrawal and are given as the difference between surface DC potential and the steady-state membrane potential without bias current injection. Membrane time constants were obtained from small hyperpolarizing current pulses as the time necessary to reach e^{-1} (63%) of the maximum voltage deflection. Likewise, input resistance was determined from measuring the maximal deflection of small hyperpolarizing current pulses. Spike amplitudes were taken from baseline to the peak of the action potential; spike duration was measured at half-amplitude. Periods of recordings were selected for amplitude measurements when the postsynaptic responses remained stationary, judged by the absence of a long-term trend in running averages of 20–50 responses. Unitary IPSP amplitudes were measured from baseline to peak. The corresponding noise levels were determined for the same time interval from baseline to baseline, using the pre-event interval of the same traces.

Histological processing and anatomical evaluation

With few exceptions, when depolarizing current pulses were employed, intracellular diffusion of biocytin from the electrode resulted in adequate filling of the recorded neurons. Slices were sandwiched between two Millipore filters and fixed in 2.5% paraformaldehyde, 1.25% glutaraldehyde and 15% (v/v) picric acid in 0.1 M phosphate buffer (pH 7.4), usually overnight. Following gelatine re-embedding, taking care to keep them flat, slices were re-sectioned on a vibratome at 50–60 μm thickness and processed for light and electron microscopy using the avidin-biotinylated horseradish peroxidase complex (Vector Laboratories), closely following previously described procedures (Halasy and Somogyi, 1993; Han *et al.*, 1993; Buhl *et al.*, 1994b). Following their embedding into epoxy resin all recovered interneurons with extensive axonal filling were scrutinized in the light microscope to establish preliminary classification according to their salient morphological features (see Results). In three instances (see Figs 2 and 3) both pre- and postsynaptic cells were graphically reconstructed from serial 60 μm sections using a light microscope and drawing tube at ×1250 magnification. Subsequently portions of the axonal arbor of all tentatively identified basket cells were re-embedded for electron microscopy (for details see Somogyi and Takagi, 1982). Labelled terminal branches of the axon were traced in serial ultrathin sections to determine their postsynaptic targets. Apart from one cell (n = 9 contacts), for each presynaptic basket cell a minimum of 10 synaptic contacts were rigorously identified. On two occasions, where a single pyramidal cell could be unequivocally allocated to a physiological recording with the characteristics of a principal cell, putative sites of synaptic interaction were mapped in the light microscope and subsequently scrutinized in serial electron microscopic sections (Fig. 4).

Results

Physiological properties of pre- and postsynaptic cells

The data presented below are based on a total of 14 physiologically as well as anatomically identified basket cells which elicited unitary IPSPs in 24 pyramidal cells, the discrepancy of numbers being due to the fact that in several instances paired recordings were obtained between a single presynaptic neuron and several successively recorded principal cells. No attempt was made to precisely determine the number of paired recordings without obvious signs of synaptic coupling. On a subjective basis, however, it appeared that the overall proportion of inhibitory interactions was relatively high, in the range of 20–50%, once a stable recording had been obtained from a cell which displayed the physiological properties of an as yet morphologically unidentified interneuron.

Basket cells had a mean resting membrane potential of –64.0 ± 5.5 mV and non-overshooting action potentials with an amplitude of 60.0 ± 8.0 mV, whereas pyramidal cells had a slightly less negative resting membrane potential of –61.0 ± 5.4 mV and overshooting action potentials (73.9 ± 6.4 mV). The average action potential duration of basket cells (0.376 ± 0.118 ms) was considerably shorter than in pyramidal cells (0.948 ± 0.179 ms). Basket cells had a mean input resistance of 48.1 ± 31.6 MΩ versus 58.2 ± 19.0 MΩ in pyramidal cells and a mean time constant of 11.2 ± 8.2 ms, which was shorter than that of pyramidal cells (15.9 ± 3.7 ms). When the physiological properties of pre- and postsynaptic cells were compared with a non-parametric statistical test (Mann–Whitney U-test) three parameters were found to be significantly different: membrane time constant ($P < 0.02$), action potential amplitude ($P < 0.0005$) and action potential duration ($P < 0.0001$). In contrast, resting membrane potential and input resistance did not differ significantly ($P > 0.05$).

In contrast to the obvious differences between basket and pyramidal cell properties, it must be emphasized that it was not feasible to

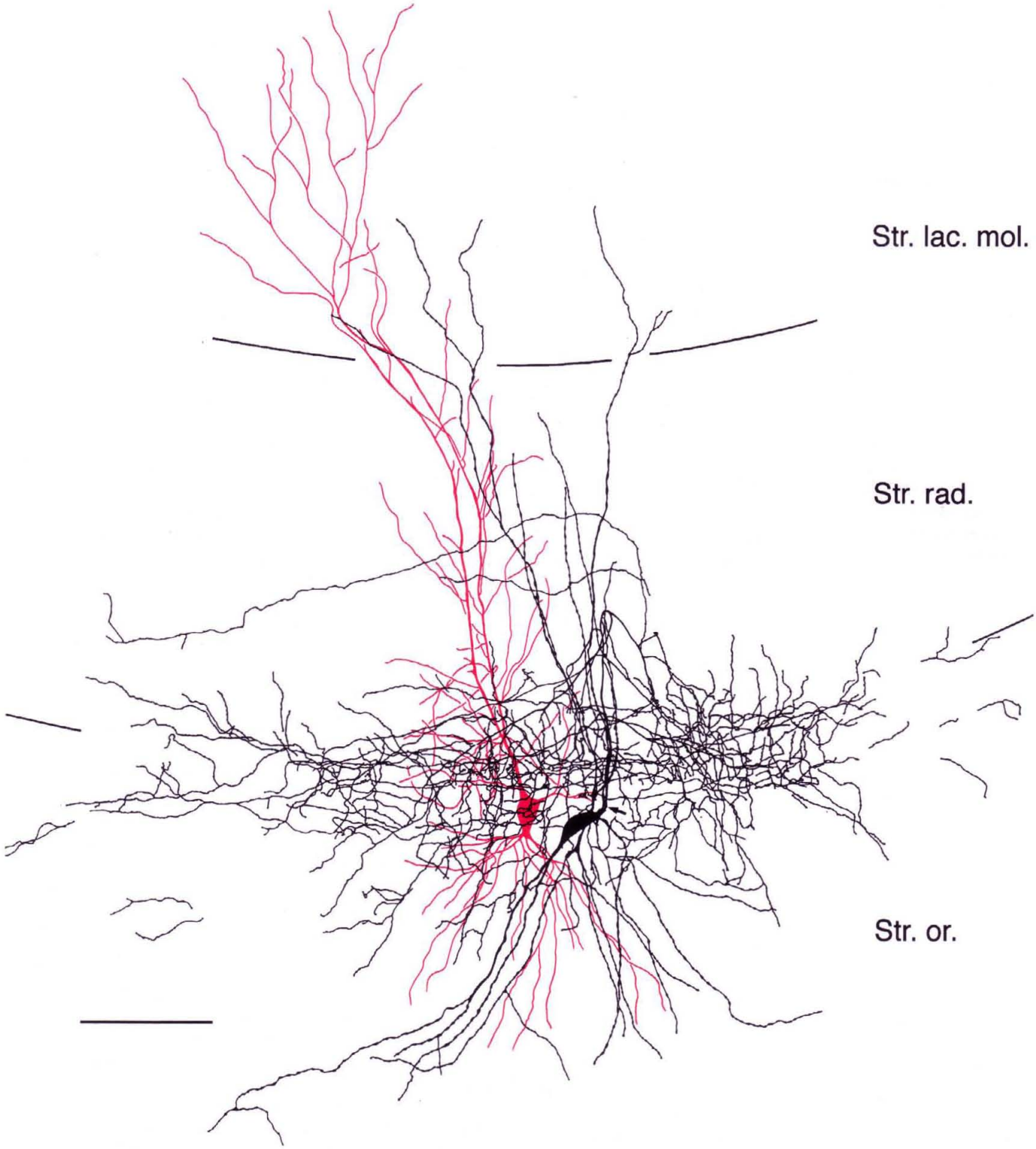

FIG. 2. Light microscopic reconstruction of a synaptically connected and intracellularly labelled basket/pyramidal cell pair. Both cells were identified by their distinctive firing patterns (shown in Fig. 1A, B). The basket cell (soma, dendrites and axonal arbor shown in black; spines not shown) elicited a short-latency fast IPSP (Fig. 1D, E) in the postsynaptic pyramidal cell (dendrites and cell body displayed in red). The inhibitory axon emerged from the basket cell soma (arrow) and densely ramified within the cell body layer and the adjacent portions of the strata radiatum (Str. rad.) and oriens (Str. or.). The border of the strata radiatum and pyramidale is indicated by the lines at the left and right. Although basket cell dendrites, as a general rule, enter the stratum lacunosum moleculare (Str. lac. mol.) they do not give rise to a prominent apical tuft. Following light microscopic analysis, the synaptic target profile of the inhibitory cell was assessed by means of random electron microscopic bouton sampling. From a total of 61 labelled boutons 29 (48%) were found in synaptic contact with somata and 2 (3%) on spines, whereas the remainder (n = 30; 49%) formed synapses with dendrites. Scale bar = 100 μm.

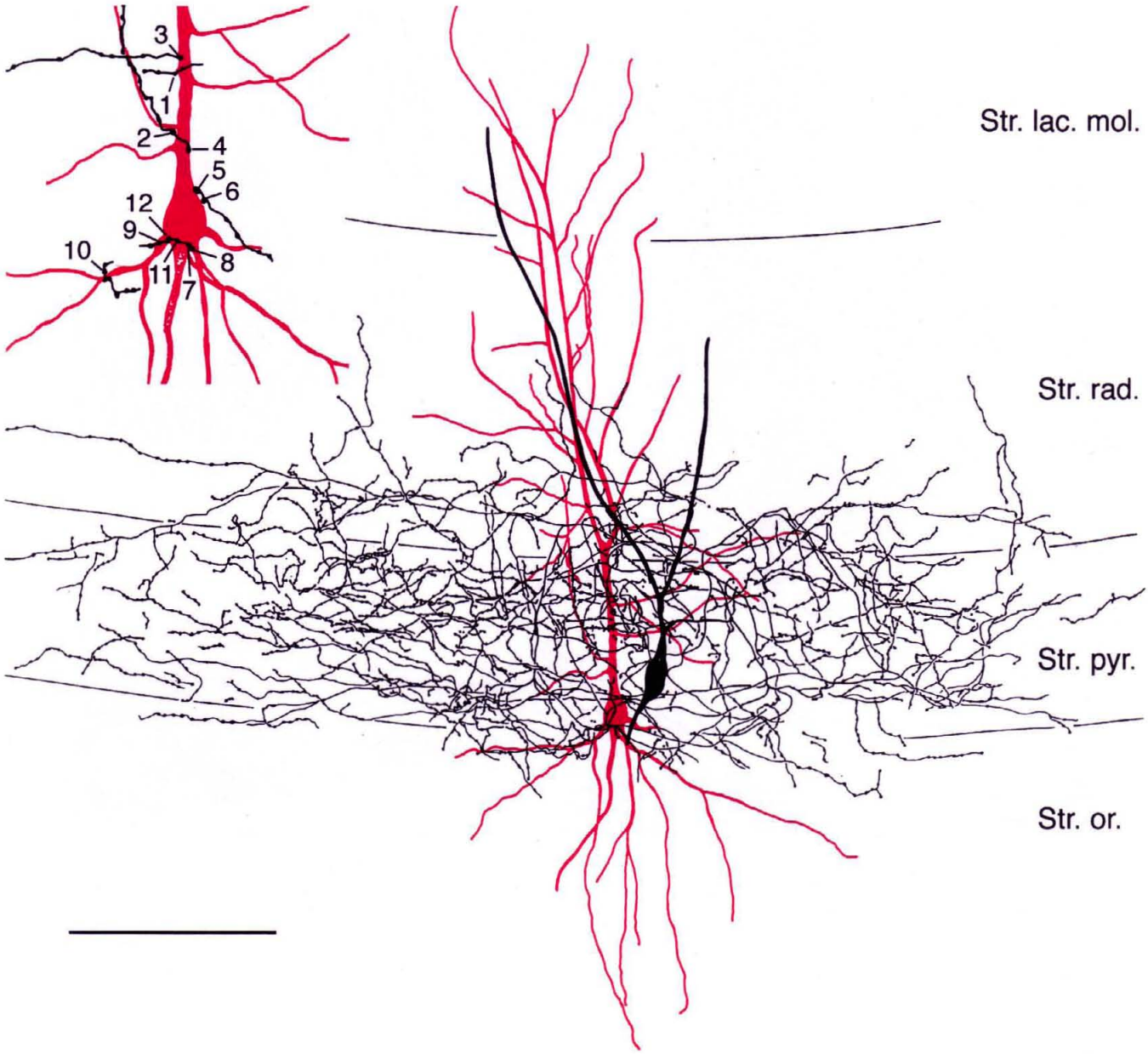

FIG. 3. Intracellularly labelled basket/pyramidal cell pair and electron microscopically determined sites of synaptic interaction. The light microscopic drawing shows the basket cell (soma, dendrites and axon in black) in close proximity to the postsynaptic pyramidal cell. Due to the loss of biocytin the basket cell dendritic tree is incomplete. The main inhibitory axon branched repeatedly and filled the pyramidal layer (Str. pyr.) and small parts of the adjacent strata radiatum (Str. rad.) and oriens (Str. or.) with a dense cloud of terminal branches. The inset shows the position of the 12 labelled basket cell terminals which were shown by electron microscopy to form synaptic junctions with the postsynaptic pyramidal cell. For electron microscopic evidence of labelled release sites see Figure 4. For the amplitude distribution of IPSPs evoked in this pyramid see Figure 7F. Str. lac. mol. = stratum lacunosum moleculare; scale bar = 100 μm.

discriminate reliably, on physiological grounds, between the different types of local-circuit neuron which reside in the pyramidal cell layer of area CA1 (see also Buhl *et al.*, 1994a). Stringent anatomical verification was therefore considered essential and recordings without adequate morphological recovery (for criteria see below) were therefore not analysed.

Anatomical definition of CA1 basket cells

Throughout much of the literature it appears that the term 'basket cell' is frequently used as a rather ill-defined denominator for a variety of GABAergic local-circuit neurons which reside in and around the cell body layer of the hippocampus. Intracellular labelling of these neurons has, however, revealed that they generally fall into fairly well defined categories, largely determined by the target selectivity of their axonal output (e.g. Somogyi *et al.*, 1983, 1985; Halasy and Somogyi, 1993; Han *et al.*, 1993; Buhl *et al.*, 1994a). Basket cells, as originally described by Ramon y Cajal (1893) and Lorente de No (1934), have much of their axon confined to the principal cell layer and its immediate surround. The terminal branches of several such cells may form pericellular 'baskets' around the somata of principal cells. However, since axo-axonic cells in Ammon's

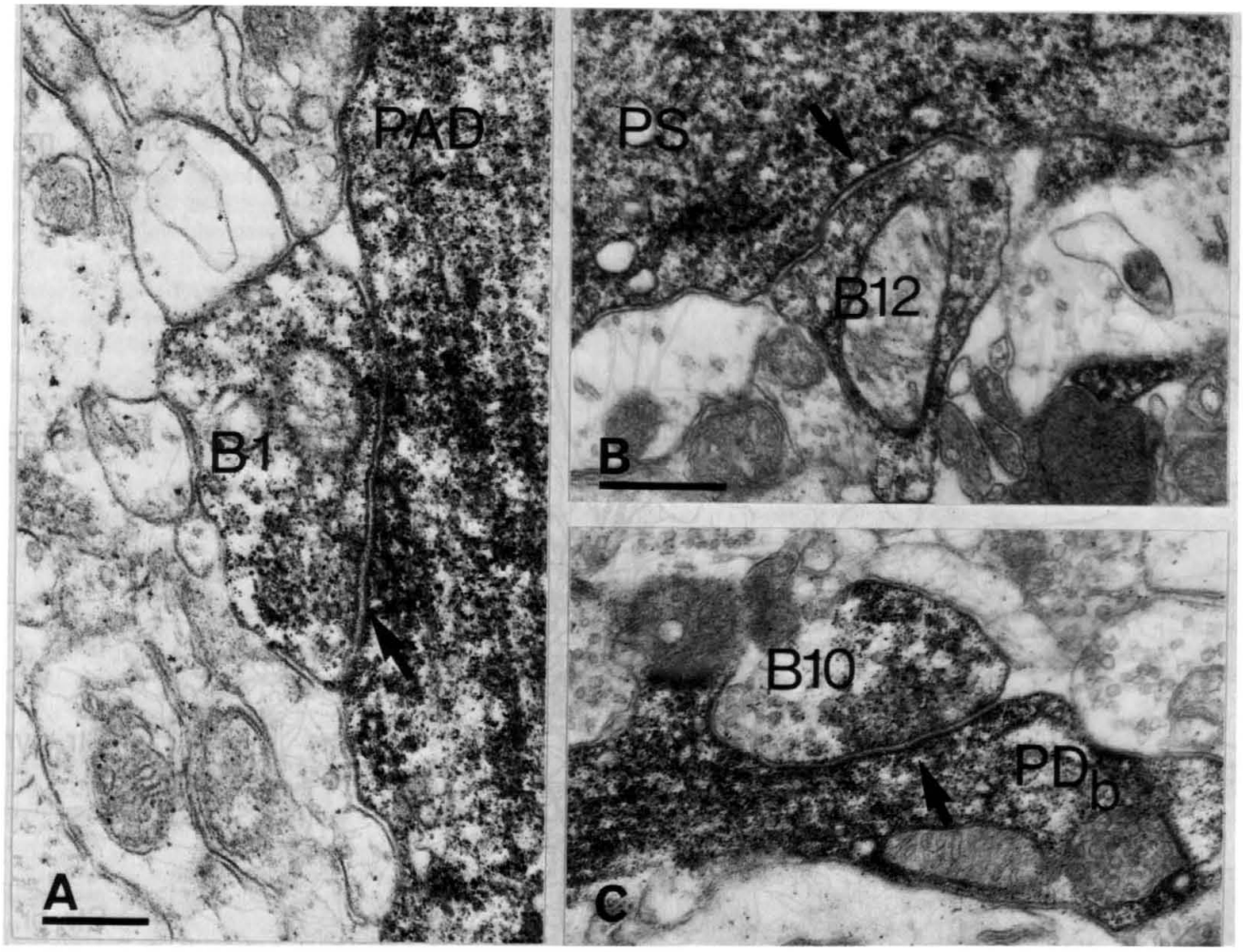

FIG. 4. The ultrastructural correlate of physiologically characterized release sites. Pre- and postsynaptic elements are discernible due to their content of electron-dense peroxidase reaction end product. The electron micrographs show three of the 12 labelled basket cell boutons which were illustrated in the previous figure. All basket cell terminals were in type 2 symmetrical contact (arrows) with the postsynaptic pyramidal cell. (A) Bouton 1 (B1) was found to be in synaptic contact with the pyramidal cell apical dendrite (PAD). (B) Terminal 12 (B12) is an example of the five synaptic contacts the basket cell established on the pyramidal cell soma. (C) The bouton denoted as 10 (B10) established a synapse with a second-order basal dendrite. Note the clearly discernible synaptic vesicles in the basket cell terminals and the widening of the extracellular space at the synaptic junctions (arrow). Scale bars = 0.2 μm in (A); 0.4 μm in (B) for (B) and (C).

horn (Somogyi *et al.*, 1985; Gulyas *et al.*, 1993b; Buhl *et al.*, 1994b) may have a similar axonal arborization pattern, more stringent criteria were therefore required to unambiguously identify particular classes of local-circuit cells (Somogyi *et al.*, 1983, 1985; Gulyas *et al.*, 1993b; Halasy and Somogyi, 1993). In the present study basket cells were thus more rigorously defined as *GABAergic interneurons with a synaptic target profile enriched in somatic contacts* (>30%). In this respect, basket cells differ from other local-circuit neurons, for example axo-axonic or bistratified cells, which very rarely terminate on principal cell bodies (Buhl *et al.*, 1994a).

Morphological features of basket cells

Biocytin-labelled basket cells in the Ammonic subfields gave rise to several primary dendrites that dichotomously branched into secondary and tertiary processes which fanned out into the strata radiatum and lacunosum moleculare as well as oriens (Fig. 2). Most of the dendrites were predominantly smooth and beaded, only rarely displaying a few spines. Provided the cells were sufficiently well labelled (10 of 14 cells), most of the apical dendrites could be traced into the stratum lacunosum moleculare but rarely branched there, thus differing from axo-axonic cells, which frequently form a prominent apical tuft (Li *et al.*, 1992; Buhl *et al.*, 1994b). As a general feature, basket cell basal dendrites deeply invaded the alvear white matter, thus differing from concomitantly recorded pyramidal cells which have their basal dendrites predominantly contained within the stratum oriens.

The axon of basket cells usually emerged from the cell body and ascended into the stratum radiatum, where it branched repeatedly into several major, frequently myelinated (data not shown) branches which then proceeded along the cell body layer. After successive further branching, preterminal and terminal axons then formed a dense meshwork of fibres criss-crossing the cell body layer and proximal regions of the strata radiatum and oriens. In the light microscope, varicose axons frequently appeared to be wrapped around unlabelled cell bodies and/or followed the initial portion of the proximal apical dendrites. The proximal apical dendrite seems to be a preferred site of terminations, as evident from the accumulation of varicose branches at the border of strata radiatum and pyramidale (Figs 2 and 3). What

TABLE 1. Location of electron microscopically determined synaptic junctions made by randomly selected labelled basket cell boutons on unlabelled postsynaptic targets

Basket cell	Area	Number of tested synapses (n)					Relative proportion of synapses (%)				
		AIS*	Soma	Dendrite	Spine	Total	AIS	Soma	Dendrite	Spine	Total
1	CA3	3	6	6	2	17	18	35	35	12	100
2	CA1	0	5	7	0	12	0	42	58	0	100
3	CA1	0	19	18	0	37	0	51	49	0	100
4	CA1	0	17	19	5	41	0	42	46	12	100
5	CA1	0	7	5	0	12	0	58	42	0	100
6	CA3	0	14	2	0	16	0	87.5	12.5	0	100
7	CA1	0	5	6	0	11	0	45.5	54.5	0	100
8	CA1	0	29	30	2	61	0	48	49	3	100
9	CA1	0	4	7	0	11	0	36	64	0	100
10	CA1	0	5	6	0	11	0	45.5	54.5	0	100
11	CA1	0	5	5	0	10	0	50	50	0	100
12	CA1	4	10	9	1	24	17	42	37	4	100
13	CA1	0	5	5	0	10	0	50	50	0	100
14	CA1	2	5	2	0	9	22	56	22	0	100
Total		9	136	127	10	282	3.2	48.2	45	3.6	100

*AIS = axon initial segment.

has been described in Golgi studies as 'pericellular nests or baskets' is rarely evident, as this peculiar phenomenon may be attributed to the bulk impregnation of up to 25 individual basket cell axons, which were recently estimated to converge on a single postsynaptic cell (Buhl *et al.*, 1994a).

Postsynaptic targets of basket cells

Postsynaptic recordings which displayed the physiological properties of principal cells could invariably be allocated to an individually labelled or a cluster of biocytin-filled pyramidal cells. In six instances, a single pyramidal cell could be unequivocally matched with the placement of the second microelectrode, whereas this proved to be impossible for the remainder of cases. To some extent, the occurrence of multiple labelling could be attributed to the fact that during the course of the experiment several neurons with the characteristics of pyramidal cells were impaled in succession. In the remainder of the cases, however, a cluster of 2–4 pyramidal cells was recovered, even when only one postsynaptic cell had been recorded. In the absence of any obvious electrical coupling, this form of multiple labelling was therefore interpreted, in agreement with previous reports, as resulting from the diffusion and/or uptake of biocytin into adjoining cells which had been damaged by the recording electrode (Gulyas *et al.*, 1993b; Buhl *et al.*, 1994b).

In the electron microscope, biocytin labelled basket cell boutons were readily discernible due to their content of an opaque reaction product (Fig. 4A–C). Vesicle-containing terminals were followed in serial electron microscopic sections to determine their postsynaptic targets. Synaptic junctions were identified on the basis of the rigid apposition of pre- and postsynaptic membrane, the widening of extracellular space at the synaptic cleft, the slightly electron-dense cleft material, the presence of presynaptic vesicles and, finally, the postsynaptic density, when detectable. All basket cells made type 2 (symmetrical) efferent synapses (Gray, 1959; Blackstad and Flood 1963). Electron microscopic analysis of a random sample of basket cell synaptic junctions (n = 282) showed that they predominantly targeted cell bodies (48.2%) and proximal dendrites (45%), in roughly equal proportions. In contrast, axon initial segments (3.2%) and spines (3.6%) formed a relatively minor proportion of postsynaptic targets (for details see Table 1).

Whenever a single postsynaptic pyramidal cell had been recovered (n = 6), the cell body and proximal dendrites were enmeshed in a tangle of basket cell axons. Without exception, light microscopical estimates revealed several sites of close membrane apposition between basket cell terminals and postsynaptic target. A precise prediction, however, proved to be impossible because, for example, portions of the basket axon were visually occluded by the opaque pyramidal soma. In two instances (basket cell 1 in Figs 3 and 4; for another example see figs 1 and 5 in Buhl *et al.*, 1994a) electron microscopic serial sections were therefore employed to systematically scrutinize the entire cell body as well as each suspect dendritic target site, where an axonal branch appeared to either cross or terminate. Thus it was found that the two postsynaptic pyramidal cells received 12 and 10 synaptic contacts respectively. Pyramidal cell 1 received seven dendritic and five somatic synapses (Fig. 3), whereas in the second example the pyramidal cell body and dendrites received five synapses each. Evidently the proportion of postsynaptic targets on these individual pyramids is also in good correspondence to the overall random synaptic target pattern of the respective presynaptic cells. Although both pyramidal cells received about half of the basket cell terminals on dendrites, these were in close proximity (<60 μm) to the cell body.

Properties of unitary basket cell-mediated IPSPs

To determine the parameters of unitary IPSPs, presynaptic cells were made to fire single action potentials (Fig. 1C) by means of either depolarizing constant or pulsed current injection at frequencies near 1 Hz. In view of the inherently low signal/noise ratios, postsynaptic responses were averaged prior to measurements (Fig. 1D, E). Moreover, postsynaptic cells were frequently depolarized with constant depolarizing current to increase the magnitude of the effect.

At an average membrane potential of –57.8 ± 4.6 mV, unitary IPSPs had a mean amplitude of 450 ± 238 μV (n = 23), ranging from 124 to 919 μV. The events had a 10–90% rise of 4.6 ± 3.2 ms (n = 18) and, measured at half-amplitude, a mean duration of 31.6 ± 18.2 ms (n = 22). Generally larger effects tended to have longer rise-times and durations. In most instances (n = 19) the decay phase of unitary IPSPs could be adequately fitted with a single exponential function (Fig. 1E) with a mean time constant of 32.4 ± 18.0 ms.

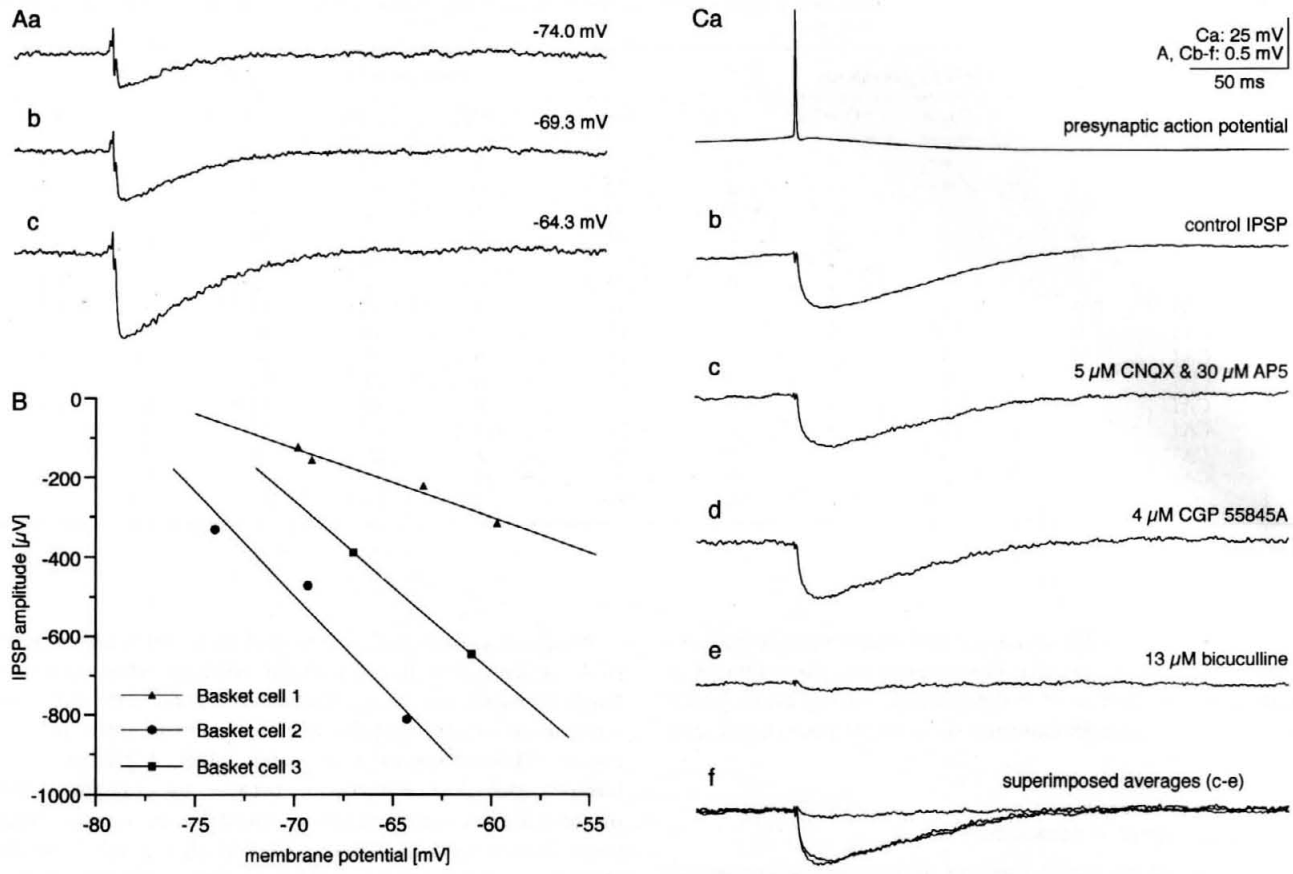

FIG. 5. Voltage dependence of IPSPs and their pharmacological properties. (A) Voltage dependence of a unitary basket cell IPSP. Whenever tested, membrane depolarization in postsynaptic pyramidal cells resulted in the successive increase of IPSP amplitudes (Aa–c). (B) Estimation of IPSP response reversal. Linear regression was employed to fit graphs to the data points and calculate the response reversal of IPSPs. (C) Pharmacological dissection of unitary basket cell IPSP. Using DC current injections the presynaptic cell was made to fire (Ca), whilst the postsynaptic membrane potential was maintained at –55 ± 1 mV throughout the experiment. (Cb) Once a stable, synaptically connected pair had been obtained the control response was followed for several minutes until superfusion with the excitatory amino acid blockers CNQX and AP5 was commenced. (Cc) Basket cell-evoked unitary IPSP following bath application of glutamate receptor antagonists. (Cd) Addition of the selective $GABA_B$ receptor antagonist CGP 55845A resulted in a marginal (4%) increase of the IPSP amplitude. (Ce) Superfusion of the $GABA_A$ receptor antagonist bicuculline, however, almost completely eliminated the response. (Cf) Superimposition of the averages shown in (Cc–e) reveals that the $GABA_B$ antagonist had only a marginal effect on the amplitude whereas the decay phase of the basket cell-evoked IPSP remained unchanged. All traces shown in (A) and (C) represent the averages of >50 sweeps.

Likewise, single exponentials were fitted to the decay phase of averages of small (–0.1 nA) current pulses delivered through the recording electrode. With one exception, the injected currents decayed with shorter time constants (20.5 ± 9.5 ms) than the respective IPSPs elicited in the same cells. This difference was statistically significant (Mann–Whitney *U*-test; $P < 0.025$).

Voltage dependence and conductance of unitary IPSPs

In all cells tested ($n = 5$) amplitudes of averaged IPSPs decreased at more hyperpolarized membrane potentials (Fig. 5A). The relationship between membrane voltage and IPSP amplitudes was approximately linear (Fig. 5B). Therefore, linear regression was employed to calculate the point of response reversal which, on average, was –74.9 ± 6.0 mV ($n = 5$). In this respect it should, however, be emphasized that this correlation may only hold for the range of membrane potentials investigated, as previous work indicates increasing non-linearities beyond the point of response reversal (Collingridge *et al.*, 1984; Miles, 1990).

Under current clamp recording conditions, an estimate of the average IPSP conductance, G_{IPSP}, may be obtained using a procedure originally derived from Ginsborg (1973) and subsequently adopted by others (for details see Miles and Wong, 1984; Benardo, 1994). In brief, using the experimentally determined values for input resistance and the slope of the IPSP amplitude–membrane voltage relationship (Fig. 5B), the mean unitary IPSP conductance was estimated to be 0.95 ± 0.29 ns, ranging from 0.52 to 1.16 ns.

Receptor pharmacology of unitary IPSPs

The pharmacological profile of unitary basket cell IPSPs was investigated in three instances. Before drug application, the control IPSPs (ranging from 141 to 476 μV) were monitored for a 10 min period to ascertain whether they remained stationary (Fig. 5Cb). Throughout the entire procedure presynaptic cells were made to discharge at 1 Hz and the pyramidal cell membrane potentials were manually adjusted with small DC current injections to remain constant, generally not deviating in excess of ±1 mV. Initially, the slices were superfused with a mixture of the non-*N*-methyl-D-aspartic acid (non-NMDA) receptor antagonist CNQX (5 or 10 μM) and the NMDA receptor antagonist AP5 (30 μM; Fig. 5Cc). In the presence of the excitatory amino acid blockers, the responses showed a small but consistent

increase in amplitude (8.3 ± 2.5% change of normalized amplitudes). Following addition of the $GABA_B$ receptor antagonist CGP 35845A [1 μM (n = 1) or 4 μM (n = 2)] to the bath, a further average increase of 26.3 ± 19.9% of the normalized mean IPSP amplitudes was observed. It is, however, noteworthy that the increase in response amplitude was largely confined to two cells [37.5% (33 and 42%)], whereas in the third example the monitored increase (4%; Fig. 5Cd, f) was marginal. In all instances, superimposition of the traces obtained in the presence of the excitatory amino acid blockers and following addition of the $GABA_B$ receptor antagonist revealed that the decay of the averaged IPSPs remained virtually unchanged (Fig. 5Cf). Finally, addition of bicuculline (10 or 13 μM) reduced the amplitude to 15.5 ± 3.1% of the response obtained in the presence of excitatory amino acid blockers. Neuronal input resistances (all cells >40 MΩ) were monitored throughout and showed only minor fluctuations.

Summation of IPSPs and use-dependent depression

High-frequency trains of presynaptic discharge (Fig. 6Aa) invariably resulted in an initial summation of the postsynaptic response (n = 5; Fig. 6Ab, c). Up to four IPSPs were effective in approximately doubling the amplitude of single action potential-triggered events. The first IPSP usually resulted in the largest amplitude increase, whereas the contribution of successive events decreased. Then, despite maintained presynaptic activity, the response remained stationary, until it gradually declined and eventually reached a steady-state level (Fig. 6Ab).

The phenomenon of frequency-dependent tonic depression was further investigated at lower presynaptic firing rates. The results illustrated in Figure 6Bb, c indicate that presynaptic firing rates in the range of 1 Hz may already result in a depression of the postsynaptic response. In the example illustrated (Fig. 6B) an ~10-fold increase of the presynaptic firing rate resulted in a >50% reduction of the IPSP amplitude (Fig. 6Be).

Amplitude distribution of unitary IPSPs

The amplitudes of unitary IPSPs appeared to fluctuate at all connections tested, although much of the intrinsic variability of the signal may have been due to the superimposition of recording noise. In several instances, when the limited number of sweeps precluded the construction of amplitude histograms, superimposition of successive events already indicated a low number or complete absence of release failures (Fig. 7B, C). Moreover, the amplitude of individual events seemed to fluctuate considerably around the average of the postsynaptic response (Fig. 7B, D).

On several occasions recordings were obtained at a given membrane potential containing a sufficiently large number of sweeps with events whose averaged amplitudes remained unchanged over time and generally exceeded that of the recording noise. From these, a total of four were selected to construct amplitude histograms. For the unitary interactions shown in Fig. 7F, G the number of release sites, as predicted from the electron microscopically defined synaptic junctions, was 12 and 10 respectively; for the remainder it was unknown. Three pairs (Fig. 7F–H) were located in area CA1 and one in subfield CA3 (Fig. 7I). In all four interactions the mean amplitude (720 ± 110 μV) was very close to the respective median (706 ± 100 μV). Individual events could be large (in three cells >2 mV peak amplitude). In contrast, very small events appeared to be rare, although the marked overlap of the signal and noise distributions (mean ± SD of noise = 294 ± 93 μV) precluded the unequivocal identification of individual response failures. The absence of a distinct peak in the 0 mV region

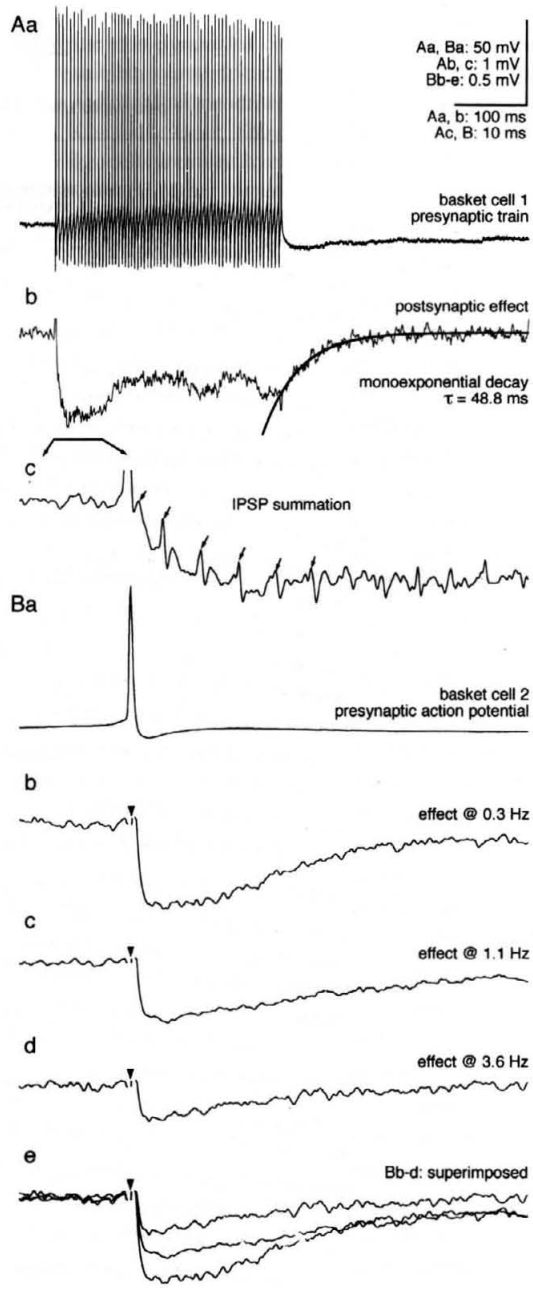

FIG. 6. Summation of IPSPs and frequency dependent attenuation. (Aa) A 300 ms train of presynaptic action potentials in a basket cell firing at a non-decrementing frequency >200 Hz. (Ab) The average of eight postsynaptic events in a pyramidal cell revealed an early peak of the response that subsequently declined and levelled at slightly more than half of the peak amplitude. Note the monoexponential decay of the IPSP, which was similar to the decay of single action potential-evoked IPSPs. (Ac) Expansion of the early response (time window indicated by horizontal bar) shown in (Ab). Because of the small variability of interspike intervals in the presynaptic cell the first six action potentials (arrows indicate coupling artefacts) superimpose precisely. It is apparent that the peak response is due to the summation of, on average, four IPSPs, with some degree of variability in individual events (data not shown). In (b) and (c) electrode-coupling artefacts caused by capacitive transients in (a) were clipped for clarity of display. (B) The presynaptic rate of discharge may affect the magnitude of the postsynaptic response. A twelvefold increase in presynaptic firing frequency from 0.3 (Ab) to 3.6 Hz (Ad) resulted in a >50% decrease of the IPSP amplitude. (Ae) Superimposition of traces (Ab–d). Arrowheads indicate position of spike capacitive artefacts which were removed for clarity. All traces in (B) represent averages of >50 responses.

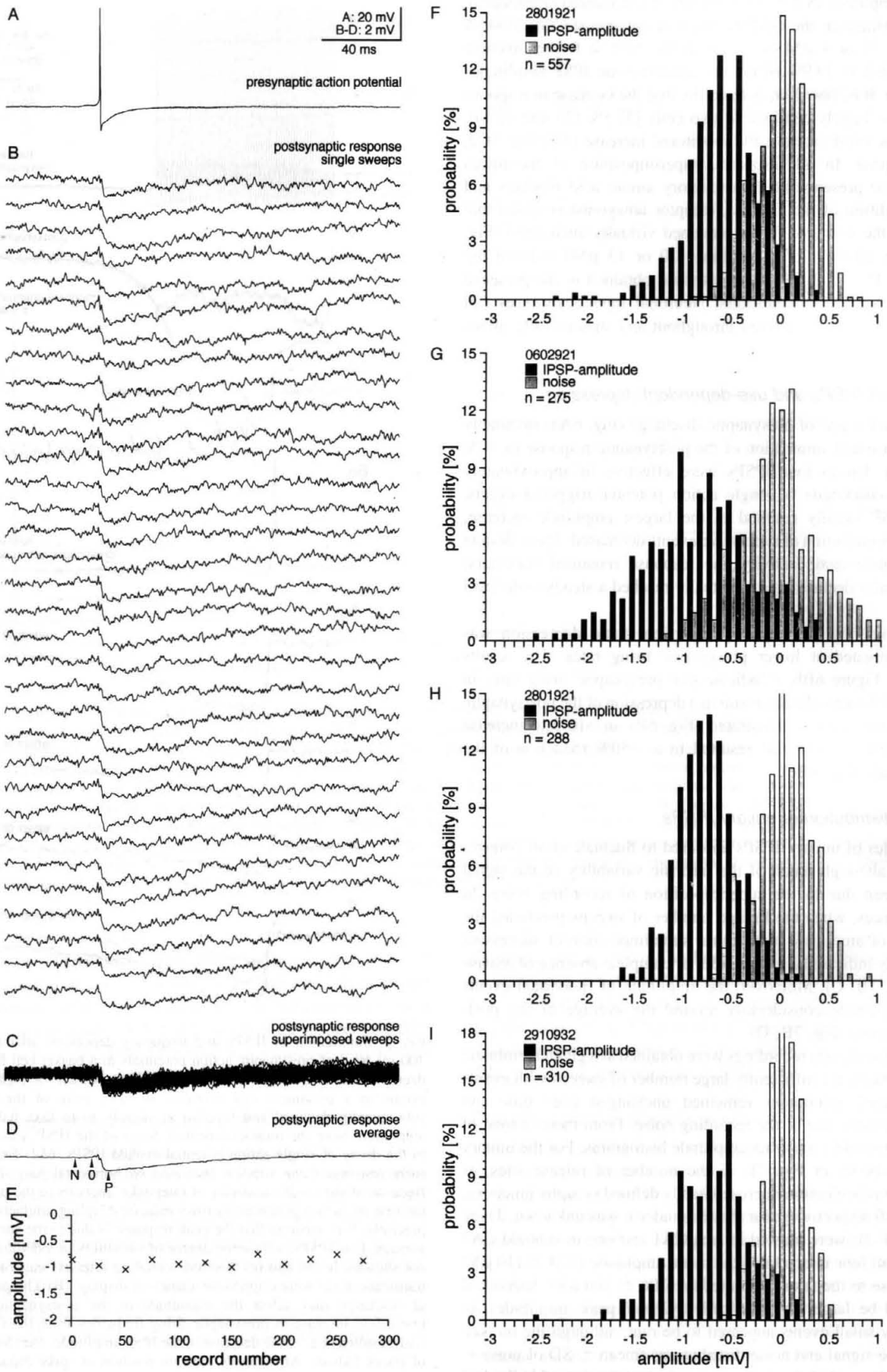
A
A: 20 mV
B-D: 2 mV
40 ms
presynaptic action potential
B
postsynaptic response
single sweeps
C
postsynaptic response
superimposed sweeps
D
postsynaptic response
average
N
0
P
E
amplitude [mV]
record number
F
2801921
IPSP-amplitude
noise
n = 557
G
0602921
IPSP-amplitude
noise
n = 275
H
2801921
IPSP-amplitude
noise
n = 288
I
2910932
IPSP-amplitude
noise
n = 310
probability [%]
amplitude [mV]

of the amplitude histogram would, however, suggest a relatively small number of response failures. Finally, a relative measure of the unitary IPSP fluctuation was obtained by determining the ratio between the variances of IPSP amplitudes and recording noise. Without exception, ranging from 1.2 to 4.1 (mean 2.3 ± 1.6), the variance of the unitary IPSPs exceed that of the baseline noise.

Postinhibitory facilitation and rebound action potentials

When elicited by single action potentials or brief bursts of basket cell discharge, the averaged postsynaptic response of four pyramidal cells was followed by a distinct depolarizing overshoot, here referred to as postinhibitory facilitation. The respective IPSPs had a mean amplitude of 414 ± 344 μV and were followed by a depolarizing wave which, on average, went 210 ± 219 μV above the pre-event baseline level. When measured from single action potential-elicited averages, the humps attained their maximum positivity at 130 ± 33 ms after the presynaptic action potential.

All postsynaptic cells had overshooting action potentials and appeared to be, in physiological terms, healthy cells (mean action potential amplitude 77 ± 7 mV; input resistance 51 ± 19 MΩ). Interestingly, all cells which displayed postinhibitory action potentials had been depolarized to membrane potentials close to the firing threshold (–54.4 ± 1.6 mV) and were seen to sporadically discharge action potentials. To some extent, due to the limited sample size, the difference in membrane potential of basket cell effects with versus those without a depolarizing hump (–59 ± 4.6 mV) was not statistically significant (Mann–Whitney *U*-test; $P = 0.088$).

Averages of postsynaptic effects such as the one shown in Figure 8B were obtained by excluding sweeps which were contaminated by action potentials. Subsequently a complementary approach was adopted by excluding from a string of successive sweeps all events when the hump was subthreshold and additionally only those where the pyramidal cell discharge preceded the basket cell action potential by <70 ms. When superimposing the remaining events it is apparent that the distinctive clustering of pyramidal cell action potentials is highly non-random and appears to temporally coincide with the occurrence of post-inhibitory facilitation (Fig. 8C, E).

Discussion

Identification of pre- and postsynaptic neurons

There is a general consensus throughout the literature that it is possible to discriminate hippocampal GABAergic local-circuit neurons due to their distinctive firing properties, such as short-duration action potentials, fast membrane time constants and non-accommodating firing pattern. The results presented above for one subclass, the basket cells, are clearly in support of this notion, as every presumed interneuron was (i) shown to elicit short-latency GABAergic IPSPs in postsynaptic principal cells; (ii) light microscopically identified as a smooth dendritic non-pyramidal cell; and (iii) shown by electron microscopy to establish symmetrical synaptic contacts predominantly with the somata and proximal dendrites of their respective postsynaptic target cells. It is equally clear, however, that membrane and firing properties of basket cells are insufficient criteria by which to discriminate them from several other types of GABAergic interneurons. Amongst those are axo-axonic cells, which have relatively few distinctive physiological features, such as spike doublets, that would allow their unequivocal discrimination from hippocampal interneurons that reside within or close to the hippocampal cell body layers (Buhl *et al.*, 1994b). It is noteworthy, however, that this notion of similarity in membrane and firing properties does not necessarily apply to all hippocampal interneurons, as, for example, stratum lacunosum moleculare interneurons do not belong to the physiologically defined group of fast spiking cells (Kawaguchi and Hama, 1988; Lacaille and Schwartzkroin, 1988).

Therefore, the apparent similarity of interneuronal membrane and firing properties is a relatively poor indicator of their connectional heterogeneity. Consequently, until better discriminatory features can be routinely exploited in conjunction with intracellular recording experiments, morphological identification of cells remains a necessity when addressing the specific roles of hippocampal interneurons. Moreover, the occasionally deceiving similarity of basket and chandelier cell axonal arbors at the light microscopic level strongly warrants the identification of the different cell types at the electron microscopic level by virtue of their distinctive synaptic target profiles. It appears, however, that the dendritic arborizations of basket and axo-axonic cells in the CA1 area are sufficiently distinct to predict the efferent synaptic targets of the respective cell type with a high degree of probability. Basket cells have more numerous radially oriented dendrites in the stratum radiatum (Buhl *et al.*, 1994a) than axo-axonic cells, whereas the latter have conspicuous tufts of dendritic branches in the stratum lacunosum moleculare (Somogyi *et al.*, 1985; Li *et al.*, 1992; Buhl *et al.*, 1994b), which is generally absent in basket cells.

The monosynaptic nature of unitary basket cell effects

Previous work by Miles (1990) has shown that the activity of a single CA3 pyramidal neuron is sufficient to elicit, via a disynaptic loop, IPSPs in a concomitantly recorded pyramidal cell. This particular mechanism involves the glutamate-evoked excitation of an interneuron brought to firing by local axon collaterals of the pyramidal cell (Miles, 1990). Such a scenario can be excluded in our recordings in view of the fact that the presynaptic cells were identified as GABAergic basket cells. Accordingly, unitary basket cell IPSPs remained unaffected in the presence of CNQX and AP5, whereas disynaptic IPSPs are diminished by excitatory amino acid blockers (Miles, 1990).

Likewise, any arguments in favour of a less well defined polysynap-

FIG. 7. Variation of unitary IPSP-amplitudes in five basket–pyramidal cell pairs. (A) presynaptic spike of a CA1 basket cell (1207941). (B) Response variability in 33 consecutively elicited pyramidal cell IPSPs. The presynaptic cell was driven at a frequency of ~1 Hz; the postsynaptic pyramidal cell was held at a membrane potential of –64 mV. (C) Superimposition of all events reveals the absence of apparent failures during this period. (D) Averaged response. Arrowheads indicate cursor positions for amplitude measurements. Noise was determined between points 0 and N, whereas IPSP amplitudes were taken, with the same time difference, between points 0 and P. (E) Plot showing running averages for the cell shown in (G). (F–H) Histograms showing IPSP amplitude distributions and baseline noise levels in three different CA1 basket–pyramidal cell pairs. The effect shown in (F) was mediated by 12 synaptic junctions (illustrated in Figs 3 and 4) whereas the one illustrated in (G) was due to the action of 10 synaptic release sites (see fig. 1 in Buhl *et al.*, 1994a). (I) Unitary basket IPSPs in a postsynaptic CA3 pyramidal cell have a similar bell-shaped amplitude distribution. Note that the amplitude histograms in (F) and (H) are derived from the same presynaptic basket cell but two successively recorded and therefore different postsynaptic neurons.

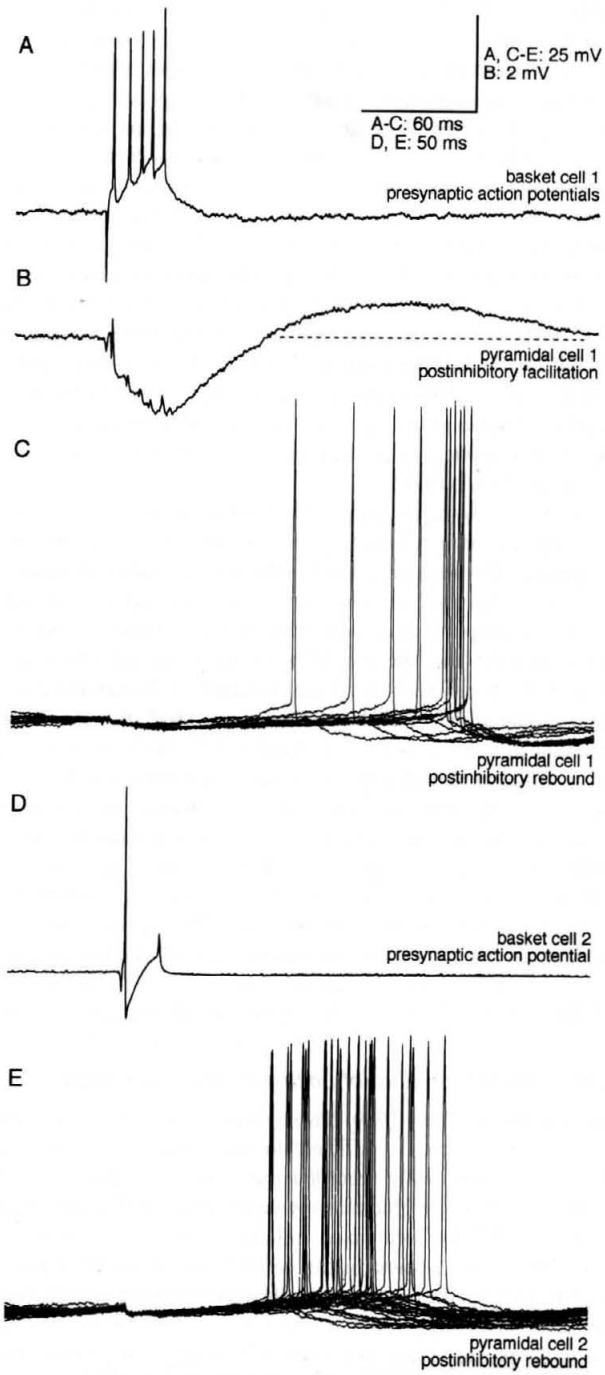

FIG. 8. Postinhibitory facilitation and rebound action potentials. (A) Brief burst of action potentials in a presynaptic basket cell. (B) Average of postsynaptic response in a synaptically coupled pyramidal cell. By passing a constant depolarizing current the pyramidal cell was held close to action potential threshold (membrane potential –54 mV) and was firing sporadically (<1 Hz). Sweeps containing pyramidal cell action potentials were excluded from this average. Note the apparent incremental summation of synaptic events (see also Fig. 6Ac) which were followed by a large amplitude 'hump' which considerably overshot the pre-event baseline level (indicated by stippled line). (C) Postinhibitory rebound action potentials. This is the same epoch of recording as shown in (B) after excluding all events in which the cell remained below the firing threshold. The superimposition of 10 consecutive sweeps reveals that the pyramidal cell preferentially discharges during the same time window in which postinhibitory facilitation was observed. (D) Presynaptic action potential, evoked by a brief depolarizing pulse, in a different basket cell. (E) Distinct clustering of consecutive rebound action potentials in the postsynaptic pyramidal cell.

tic pathway appear to be rather unlikely, since the very short latencies of basket cell IPSPs are not compatible with the inevitably longer synaptic and conduction delays required for such a hypothetical circuit. Furthermore, the probability of transmission failures would be expected to increase disproportionally with the number of synaptic links, whereas most basket cell-mediated interactions showed few if any apparent failures. Finally, irrefutable evidence in favour of a monosynaptic connection was obtained by the anatomical verification of identified basket cell terminals being in synaptic contact with two unequivocally identified postsynaptic pyramidal cells.

Unitary basket cell IPSPs—some consensus data

Paired recording techniques have been previously employed to study unitary inhibitory interactions in the major hippocampal subfields, the dentate gyrus (Scharfman *et al.*, 1990), subfield CA3 (Miles and Wong, 1984, 1987; Miles, 1990) and area CA1 (Knowles and Schwartzkroin, 1981; Lacaille *et al.*, 1987; Lacaille and Schwartzkroin, 1988). Although anatomical findings would suggest that probably most of the data are derived from a pool of heterogeneous presynaptic cells, a number of general principles have emerged that appear to govern unitary synaptic interactions: first, in most instances the probability of successfully encountering a monosynaptic connection is rather high (>0.3; Knowles and Schwartzkroin, 1981; Miles and Wong 1984; Lacaille *et al.*, 1987), thus reflecting a high degree of divergence of the local inhibitory axonal arbors. For instance, for basket cells in the CA3 area, light microscopic estimates of the bouton numbers arrived at figures ranging from 3484 to 9972 (Gulyas *et al.*, 1993b). If a basket cell were to establish, on average, 10 synaptic contacts with its postsynaptic targets, this would suggest ~350–1000 postsynaptic cells within the confines of the slice. Comparable values were recently obtained for axo-axonic cells in the CA1 area of the rat (Li *et al.*, 1992; Buhl *et al.*, 1994b). Second, as yet there appears to be no evidence for biphasic dual-component unitary IPSPs. Third, considerable variability was found not only for the average strength of different unitary connections but also for the amplitude distribution of individual events within a given connection (Miles and Wong, 1984; Miles, 1990; Scharfman *et al.*, 1990). Fourth, tetanic stimulation of the presynaptic cell generally results in the summation of several events and is followed by a subsequent decrement in the postsynaptic response (Miles and Wong, 1984; Lacaille *et al.*, 1987; Scharfman *et al.*, 1990).

Receptor pharmacology of basket cell-mediated IPSPs

The rapid onset, fast rise kinetics and the extrapolated response reversals of unitary basket cell IPSPs strongly suggest that they elicit, in concert with at least two further types of GABAergic neuron (Buhl *et al.*, 1994a), the $GABA_A$ receptor-mediated component of compound IPSPs that are commonly observed in response to the stimulation of afferent pathways (Alger and Nicoll, 1979). In marked contrast, the relatively sluggish onset of pharmacologically isolated $GABA_B$ receptor-mediated responses shows a characteristic lag of 6–8 ms, which is presumably due to a delay corresponding to the activation of postsynaptic G-proteins (Otis *et al.*, 1993). Moreover, unitary basket cell IPSPs decayed rapidly and generally monoexponentially back to baseline, approximately an order of magnitude faster than $GABA_B$ receptor-mediated potentials (Otis *et al.*, 1993). In view of the kinetic properties of basket cell-mediated IPSPs, it is not surprising that the pre- and postsynaptic $GABA_B$ receptor antagonist CGP 55845A neither decreased (for presynaptic effects see below) their amplitude nor appreciably shortened their decay. The dramatic reduction of basket cell-mediated IPSPs by bicuculline would therefore

suggest that they were exclusively mediated by the activation of $GABA_A$ receptors. These physiological results are in agreement with the immunocytochemical demonstration of the α_1 and $\beta_{2/3}$ subunits of the $GABA_A$ receptor in somatic synapses of dentate granule cells where dentate basket cells terminate (Nusser *et al.*, 1995)

Despite this seemingly straightforward interpretation of these findings it is nevertheless conceivable that a different scenario of events may lead to $GABA_B$ receptor activation, for example the spillover of GABA to extra- or perisynaptic sites (Solis and Nicoll, 1992; Isaacson *et al.*, 1993; Mody *et al.*, 1994). It is therefore of interest to note that high-frequency long-duration trains of action potentials in basket cells failed to appreciably prolong the decay of summed IPSPs. In support of these findings, the notion of separate populations of GABAergic neurons being responsible for $GABA_A$ and $GABA_B$ receptor-mediated effects has been repeatedly put forward by others. Thus, unitary IPSPs elicited by CA3 pyramidal cell layer interneurons are abolished by the $GABA_A$ receptor antagonist picrotoxin (Miles, 1990), whereas stratum lacunosum moleculare interneurons in area CA1 evoke slow IPSPs (Lacaille and Schwartzkroin, 1988), although their precise receptor mechanisms remain to be established (Williams and Lacaille, 1992). In the dentate gyrus spontaneous inhibitory postsynaptic currents (IPSCs) have been shown to selectively activate $GABA_A$ receptors (Otis and Mody, 1992). Furthermore, local application of nipecotic acid, which induces GABA release, via a heteroexchange mechanism may evoke pure $GABA_A$ or $GABA_B$ responses (Solis and Nicoll, 1992). Finally, in hippocampal neurons the potassium channel blocker 4-aminopyridine may result in the isolated appearance of either fast or slow spontaneous IPSPs (Muller and Misgeld, 1990; Misgeld *et al.*, 1992), the latter being sensitive to the $GABA_B$ receptor antagonist 2-hydroxysaclofen (Segal, 1990).

Presynaptic control of basket cell-mediated GABA release

A wealth of earlier literature indicated that GABAergic inhibition is depressed following repetitive activation of afferent pathways (e.g. McCarren and Alger, 1985; Thompson and Gahwiler, 1989; for review see Thompson, 1994). These findings, however, are sometimes difficult to interpret in view of the generally disynaptic nature of the evoked IPSPs. This disadvantage can be largely circumvented by focusing on monosynaptically elicited unitary events which permit the analysis of frequency dependent phenomena on a small number of functionally homogeneous synapses. Under these conditions we found that responses mediated by basket cell synapses show a marked frequency-dependent depression of their postsynaptic response, although the response never faded completely, regardless of the presynaptic discharge frequency. Pharmacological blockade of $GABA_B$ receptors resulted in an amplitude increase of averaged IPSPs already at presynaptic tonic firing rates in the range of 1 Hz. The most parsimonious explanation for these findings is that GABA which is released from basket cell terminals acts not only on postsynaptic $GABA_A$ receptors but also on presynaptic $GABA_B$ autoreceptors which govern neurotransmitter release (Davies *et al.*, 1990; Davies and Collingridge, 1993). It is thus possible that, to some extent, the measurements of IPSP amplitudes and calculated conductance values within this frequency range may also have been affected by the activation of presynaptic $GABA_B$ receptors. As an alternative explanation for frequency-dependent depression of IPSP amplitudes it is conceivable that chloride loading due to the bulk activation of many GABAergic synapses may lead to a change in the chloride equilibrium potential and thus to a decrease in the response amplitude (Thompson and Gahwiler, 1989). This possibility, however, seems rather remote considering that unitary events are mediated by a comparatively small number of synaptic contacts: ~4% of perisomatically positioned basket cell terminals (Buhl *et al.*, 1994a).

In line with the data emerging from the analysis of unitary events, work on pharmacologically isolated IPSPs (Davies *et al.*, 1990; Nathan and Lambert, 1991; Davies and Collingridge, 1993; Lambert and Wilson, 1993, 1994) and miniature IPSCs (Cohen *et al.*, 1992; Behrends and Tenbruggencate, 1993; Capogna *et al.*, 1993) has provided evidence for the existence of presynaptic $GABA_B$ receptors on the terminals of GABAergic interneurons (Davies and Collingridge, 1993). In addition, presynaptic opioid (Cohen *et al.*, 1992; Capogna *et al.*, 1993; Lambert and Wilson, 1993) and muscarinic receptors (Behrends and Tenbruggencate, 1993) were also shown to be involved in the regulation of transmitter release from GABAergic terminals. As yet, however, it is not clear whether anatomically distinct subsets of GABAergic interneurons may differ with respect to the expression of presynaptic receptors, as Lambert and Wilson (1993) have recently proposed.

Unitary conductance and number of release sites

In two instances it could be demonstrated that a unitary basket cell IPSP was mediated by 10 (Buhl *et al.* 1994a) and 12 synaptic contacts respectively. Previously, counts of synaptic junctions were found to be in accord with the number of release sites (n), as determined by quantal analysis (Korn *et al.*, 1982; Gulyas *et al.* 1993a). Quantal models of transmitter release assume that postsynaptic responses occur as integer multiples of an elementary synaptic event, the response to a single quantum of neurotransmitter (for review see Redman, 1990). In area CA1 the averaged GABA-mediated quantal conductance was estimated to be in the range of 258–326 pS (Ropert *et al.*, 1990), being very close to the figures which were obtained for conductance changes responsible for inhibitory quantal events in dentate granule cells (200 – 400 pS; Edwards *et al.*, 1990). These values provide an indication that, on average, unitary basket cell-mediated IPSPs may be due to the synchronous release and summation of not more than 3–4 quanta. In view of the ~3 times higher number of release sites, it would thus appear that the release probability (P) at basket cell terminals is relatively low, in the range of 0.3, thus being similar to the experimentally determined P at inhibitory synapses on the goldfish Mauthner cell (Korn *et al.*, 1982). In spite of P being low, the relatively high n nevertheless restricts the number of total transmission failures, as evidenced by the absence of a discernible failure peak in the amplitude histograms (see also Miles, 1990).

Inhibitory rebound and population synchronization

Spencer and Kandel (1961), in their pioneering *in vivo* studies, noticed that IPSPs were frequently followed by action potentials, a phenomenon to which they referred as 'rebound excitation'. They proposed that rebound excitation may be mediated either by the arrival of late EPSPs or, alternatively, by a similar mechanism such as anodal break spikes following hyperpolarizing currents. Subsequently, rebound excitation was also noted in conjunction with unitary IPSPs which were mediated by stratum lacunosum moleculare interneurons (Lacaille and Schwartzkroin, 1988). As excitatory synaptic mechanisms do not participate in the generation of unitary IPSPs it would thus appear more likely that it is the membrane hyperpolarization which is responsible for the generation of the stratum lacunosum moleculare and/or basket cell-mediated postinhibitory facilitation. Indeed, a variety of voltage dependent conductances have been described which may result in a postinhibitory overshooting membrane depolarization. Thus, facilitation may be due to the

deinactivation of sodium or calcium channels (Carbone and Lux, 1984; Stafstrom *et al.*, 1985; Llinas, 1988). Likewise, an involvement of the hyperpolarization-activated current (I_h) cannot be excluded (Halliwell and Adams, 1982; Maccaferri *et al.*, 1993).

Although the ionic basis of the depolarizing potential remains to be analysed, recent data (Cobb *et al.*, 1995) suggest a functional role for the rebound facilitation. The occurrence of postinhibitory facilitation appears to be correlated with the presence/absence of intrinsic membrane oscillations. In entorhinal and hippocampal neurons these predominate in a narrow voltage range around the action potential threshold (Alonso and Llinas, 1989; Leung and Yim, 1991; Garcia-Munoz *et al.*, 1993) and may thus serve to explain the absence of basket cell-mediated postinhibitory facilitation in CA1 pyramidal cells at more negative membrane potentials. Recent work in other systems has provided clear evidence that synaptic events, such as IPSPs, may reset the phase of intrinsic oscillations and may thus serve as a synchronizing device (Soltesz and Crunelli, 1992). As hippocampal pyramidal cells, when depolarized above firing threshold, fire predominantly on the positive phase of the oscillation (Leung and Yim, 1991; Garcia-Munoz *et al.*, 1993; Soltesz and Deschenes, 1993), it is equally likely that inhibitory events may also serve to determine the timing of action potentials (Ylinen *et al.*, 1995). Clearly, more experiments are required to analyse the effect of unitary basket cell IPSPs on intrinsic membrane oscillations and pyramidal cell firing.

A distinct functional role for basket cells?

GABAergic basket cells constitute only one of several well defined classes of hippocampal GABAergic interneurons. Amongst those, it is largely their synaptic target selectivity which renders basket cells a distinct neuronal entity. At the onset of the present study it therefore appeared reasonable to assume that it may be to some extent also their postsynaptic effect which provides the relevant cues to the specific functional role of basket cells. With respect to eliciting fast, perisomatic $GABA_A$ receptor-mediated inhibition, however, basket cells resemble axo-axonic cells (Buhl *et al.*, 1994a) which act through the same postsynaptic receptor type(s), albeit on the axon initial segment of principal cells. Although at first glance this similarity of effects may render the target specificity of perisomatic GABAergic synapses redundant, these findings do rather indicate that differences of $GABA_A$ receptor-mediated synaptic mechanisms are more subtle than currently assumed.

Acknowledgements

The authors wish to thank P. Jays, F. D. Kennedy, D. Latawiec and J. D. B. Roberts for expert technical assistance. We are grateful to O. Paulsen for critical comments on the manuscript and G. Tamas for his contribution to the light and electron microscopic analysis of some specimens. K. H. was supported by the Wellcome Trust.

Abbreviations

ACSF	artificial cerebrospinal fluid
AP5	DL-2-amino-5-phosphonopentanoic acid
CNQX	6-cyano-7-nitroquinoxaline-2,3-dione
fAHP	fast afterhyperpolarizing potential
GABA	γ-aminobutyric acid
IPSC	inhibitory postsynaptic current
IPSP	inhibitory postsynaptic potential
NMDA	*N*-methyl-D-aspartic acid

References

Aghajanian, G. K. and Rasmussen, K. (1989) Intracellular studies in the facial nucleus illustrating a simple new method for obtaining viable motoneurons in adult rat brain slices. *Synapse*, **3**, 331–338.

Alger, B. E. and Nicoll, R. A. (1979) GABA-mediated biphasic inhibitory responses in hippocampus. *Nature*, **281**, 315–317.

Alonso, A. and Llinas, R. R. (1989) Subthreshold Na^+-dependent theta-like rhythmicity in stellate cells of entorhinal cortex layer II. *Nature*, **342**, 175–177.

Andersen, P., Eccles, J. C. and Loyning, Y. (1963) Recurrent inhibition in the hippocampus with identification of the inhibitory cells and its synapses. *Nature*, **198**, 540–542.

Andersen, P., Eccles, J. C. and Loyning, Y. (1964a) Location of postsynaptic inhibitory synapses on hippocampal pyramids. *J. Neurophysiol.*, **27**, 592–607.

Andersen, P., Eccles, J. C. and Loyning, Y. (1964b) Pathway of postsynaptic inhibition in the hippocampus. *J. Neurophysiol.*, **27**, 608–619.

Baude, A., Nusser, Z., Roberts, J. D. B., Mulvihill, E., Mcilhinney, R. A. J. and Somogyi, P. (1993) The metabotropic glutamate receptor (mGluR1 alpha) is concentrated at perisynaptic membrane of neuronal subpopulations as detected by immunogold reaction. *Neuron*, **11**, 771–787.

Behrends, J. C. and Tenbruggencate, G. (1993) Cholinergic modulation of synaptic inhibition in the guinea pig hippocampus *in vitro*—excitation of GABAergic interneurons and inhibition of GABA-release. *J. Neurophysiol.*, **69**, 626–629.

Benardo, L. S. (1994) Separate activation of fast and slow inhibitory postsynaptic potentials in rat neocortex *in vitro*. *J. Physiol. (Lond.)*, **476**, 203–215.

Blackstad, T. W. and Flood, P. R. (1963) Ultrastructure of hippocampal axo-somatic synapses. *Nature*, **198**, 542–543.

Buhl, E. H., Halasy, K. and Somogyi, P. (1994a) Diverse sources of hippocampal unitary inhibitory postsynaptic potentials and the number of synaptic release sites. *Nature*, **368**, 823–828.

Buhl, E. H., Han Z.-S., Lorinczi, Z., Stezhka, V. V., Karnup, S. V. and Somogyi, P. (1994b) Physiological properties of anatomically identified axo-axonic cells in the rat hippocampus. *J. Neurophysiol.*, **71**, 1289–1307.

Capogna, M., Gahwiler, B. H. and Thompson, S. M. (1993) Mechanism of μ-opioid receptor-mediated presynaptic inhibition in the rat hippocampus *in vitro*. *J. Physiol. (Lond.)*, **470**, 539–558.

Carbone, E. and Lux, H. D. (1984) A low voltage-activated, fully inactivating Ca channel in vertebrate sensory neurons. *Nature*, **310**, 501–502.

Cobb, S. R., Buhl, E. H., Halasy, K. and Somogyi, P. (1995) GABAergic interneurons can pace hippocampal principal cell activity through perisomatic synapses *in vitro*. *J. Physiol. (Lond.)*, in press.

Cohen, G. A., Van Doze, A. and Madison, D. V. (1992) Opioid inhibition of GABA release from presynaptic terminals of rat hippocampal interneurons. *Neuron*, **9**, 325–335.

Collingridge, G. L., Gage, P. W. and Robertson, B. (1984) Inhibitory post-synaptic currents in rat hippocampal CA1 neurons. *J. Physiol. (Lond.)*, **356**, 551–564.

Davies, C. H. and Collingridge, G. L. (1993) The physiological regulation of synaptic inhibition by $GABA_B$ autoreceptors in rat hippocampus. *J. Physiol. (Lond.)*, **472**, 245–265.

Davies, C. H., Davies, S. N. and Collingridge, G. L. (1990) Paired-pulse depression of monosynaptic GABA-mediated inhibitory postsynaptic responses in rat hippocampus. *J. Physiol. (Lond.)*, **424**, 513–531.

Deller, T. and Leranth, C. (1990) Synaptic connections of neuropeptide Y (NPY) immunoreactive neurons in the hilar area of the rat hippocampus. *J. Comp. Neurol.*, **300**, 433–447.

Edwards, F. A., Konnerth, A. and Sakmann, B. (1990) Quantal analysis of inhibitory synaptic transmission in the dentate gyrus of rat hippocampal slices: a patch-clamp study. *J. Physiol. (Lond.)*, **430**, 213–249.

Garcia-Munoz, A., Barrio, L. C. and Buno, W. (1993) Membrane potential oscillations in CA1 hippocampal pyramidal neurons *in vitro*: intrinsic rhythms and fluctuations entrained by sinusoidal injected current. *Exp. Brain Res.*, **97**, 325–333.

Ginsborg, B. L. (1973) Electrical changes in the membrane in junctional transmission. *Biochim. Biophys. Acta*, **300**, 289–317.

Gray, E. G. (1959) Axo-somatic and axo-dendritic synapses of the cerebral cortex: an electron microscope study. *J. Anat.*, **93**, 420–433.

Gulyas, A. I., Gorcs, T. J. and Freund, T. F. (1990) Innervation of different peptide-containing neurons in the hippocampus by GABAergic septal afferents. *Neuroscience*, **37**, 31–44.

Gulyas, A. I., Toth, K., Danos, P. and Freund, T. F. (1991) Subpopulations

of GABAergic neurons containing parvalbumin, calbindin D28k, and cholecystokinin in the rat hippocampus. *J. Comp. Neurol.*, **312**, 371–378.

Gulyas, A. I., Miles, R., Sik, A., Toth, K., Tamamaki, N. and Freund, T. F. (1993a) Hippocampal pyramidal cells excite inhibitory neurons through a single release site. *Nature*, **366**, 683–687.

Gulyas, A. I., Miles, R., Hajos, N. and Freund, T. F. (1993b) Precision and variability in postsynaptic target selection of inhibitory cells in the hippocampal CA3 region. *Eur. J. Neurosci.*, **5**, 1729–1751.

Halasy, K., Miettinen, R., Szabat, E. and Freund, T. F. (1992) GABAergic interneurons are the major postsynaptic targets of median raphe afferents in the rat dentate gyrus. *Eur. J. Neurosci.*, **4**, 144–153.

Halasy, K. and Somogyi, P. (1993) Subdivisions in the multiple GABAergic innervation of granule cells in the dentate gyrus of the rat hippocampus. *Eur. J. Neurosci.*, **5**, 411–429.

Halliwell, J. V. and Adams, P. R. (1982) Voltage-clamp analysis of muscarinic excitation in hippocampal neurons. *Brain Res.*, **250**, 71–92.

Han, Z.-S., Buhl, E. H., Lorinczi, Z. and Somogyi, P. (1993) A high degree of spatial selectivity in the axonal and dendritic domains of physiologically identified local-circuit neurons in the dentate gyrus of the rat hippocampus. *Eur. J. Neurosci.*, **5**, 395–410.

Horikawa, K. and Armstrong, W. E. (1988) A versatile means of intracellular labeling: injection of biocytin and its detection with avidin conjugates. *J. Neurosci. Methods*, **25**, 1–11.

Isaacson, J. S., Solis, J. M. and Nicoll, R. A. (1993) Local and diffuse synaptic actions of GABA in the hippocampus. *Neuron*, **10**, 165–175.

Kawaguchi, Y. and Hama, K. (1988) Physiological heterogeneity of nonpyramidal cells in rat hippocampal CA1 region. *Exp. Brain Res.*, **72**, 494–502.

Knowles, W. D. and Schwartzkroin, P. A. (1981) Local circuit synaptic interactions in hippocampal brain slices. *J. Neurosci.*, **1**, 318–322.

Korn, H., Mallet, A., Triller, A. and Faber, D. S. (1982) Transmission at a central inhibitory synapse. II. Quantal description of release, with a physical correlate for binomial *n*. *J. Neurophysiol.*, **48**, 679–707.

Kosaka, T., Katsumaru, H., Hama, K., Wu, J.-Y. and Heizmann, C. W. (1987) GABAergic neurons containing the Ca^{2+}-binding protein parvalbumin in the rat hippocampus and dentate gyrus. *Brain Res.*, **419**, 119–130.

Kosaka, T., Kosaka, K., Tateishi, K., Hamaoka, Y., Yanaihara, N., Wu, J.-Y. and Hama, K. (1985) GABAergic neurons containing CCK-8-like and/or VIP-like immunoreactivities in the rat hippocampus and dentate gyrus. *J. Comp. Neurol.*, **239**, 420–430.

Lacaille, J.-C., Mueller, A. L., Kunkel, D. D. and Schwartzkroin, P. A. (1987) Local circuit interactions between oriens/alveus interneurons and CA1 pyramidal cells in hippocampal slices: electrophysiology and morphology. *J. Neurosci.*, **7**, 1979–1993.

Lacaille, J.-C. and Schwartzkroin, P. A. (1988) Stratum lacunosum-moleculare interneurons of hippocampal CA1 region. I. Intracellular response characteristics, synaptic responses, and morphology. *J. Neurosci.*, **8**, 1400–1410.

Lambert, N. A. and Wilson, W. A. (1993) Heterogeneity in presynaptic regulation of GABA release from hippocampal inhibitory neurons. *Neuron*, **11**, 1057–1067.

Lambert, N. A. and Wilson, W. A. (1994) Temporally distinct mechanisms of use-dependent depression at inhibitory synapses in the rat hippocampus *in vitro*. *J. Neurophysiol.*, **72**, 121–130.

Leung, L. S. and Yim, C. C. (1991) Intrinsic membrane potential oscillations in hippocampal neurons *in vitro*. *Brain Res.*, **553**, 261–274.

Li, X.-G., Somogyi, P., Tepper, J. M. and Buzsaki, G. (1992) Axonal and dendritic arborization of an intracellularly labeled chandelier cell in the CA1 region of rat hippocampus. *Exp. Brain Res.*, **90**, 519–525.

Llinas, R. R. (1988) The intrinsic electrophysiological properties of mammalian neurons: Insights into central nervous system functions. *Science*, **242**, 1654–1664.

Lorente de No, R. (1934) Studies on the structure of the cerebral cortex. II. Continuation of the study of the Ammonic system. *J. Psychol. Neurol.*, **46**, 113–177.

Maccaferri, G., Mangoni, M., Lazzari, A. and DiFrancesco, D. (1993) Properties of the hyperpolarization-activated current in rat hippocampal CA1 pyramidal cells. *J. Neurophysiol.*, **69**, 2129–2136.

Mason, A., Nicoll, A. and Stratford, K. (1991) Synaptic transmission between individual pyramidal neurons of the rat visual cortex *in vitro*. *J. Neurosci.*, **11**, 72–84.

McBain, C. J., Dichiara, T. J. and Kauer, J. A. (1994) Activation of metabotropic glutamate receptors differentially affects two classes of hippocampal interneurons and potentiates excitatory synaptic transmission. *J. Neurosci.*, **14**, 4433–4445.

McBain, C. J. and Dingledine, R. (1993) Heterogeneity of synaptic glutamate receptors on CA3 stratum radiatum interneurons of rat hippocampus. *J. Physiol. (Lond.)*, **462**, 373–392.

McCarren, M. and Alger, B. E. (1985) Use-dependent depression of IPSPs in rat hippocampal pyramidal cells *in vitro*. *J. Neurophysiol.*, **53**, 557–571.

Miettinen, R. and Freund, T. F. (1992) Neuropeptide Y-containing interneurons in the hippocampus receive synaptic input from median raphe and GABAergic septal afferents. *Neuropeptides*, **22**, 185–193.

Miettinen, R., Gulyas, A. I., Baimbridge, K. G., Jacobowitz, D. M. and Freund, T. F. (1992) Calretinin is present in non-pyramidal cells of the rat hippocampus. II. Co-existence with other calcium binding proteins and GABA. *Neuroscience*, **48**, 29–43.

Miles, R. (1990) Variation in strength of inhibitory synapses in the CA3 region of guinea-pig hippocampus *in vitro*. *J. Physiol. (Lond.)*, **431**, 659–676.

Miles, R. and Wong, R. K. S. (1984) Unitary inhibitory synaptic potentials in the guinea-pig hippocampus *in vitro*. *J. Physiol. (Lond.)*, **356**, 97–113.

Miles, R. and Wong, R. K. S. (1987) Inhibitory control of local excitatory circuits in the guinea-pig hippocampus. *J. Physiol. (Lond.)*, **388**, 611–629.

Misgeld, U., Bijak, M. and Brunner, H. (1992) *The Dentate Gyrus and its Role in Seizures*. Elsevier Science Publishers BV, Amsterdam, pp. 113–118.

Mody, I., De Koninck, Y., Otis, T. S. and Soltesz, I. (1994) Bridging the cleft at GABA synapses in the brain. *Trends Neurosci.*, **17**, 517–525.

Muller, W. and Misgeld, U. (1990) Inhibitory role of dentate hilus neurons in guinea pig hippocampal slice. *J. Neurophysiol.*, **64**, 46–56.

Nathan, T. and Lambert, J. D. (1991) Depression of the fast IPSP underlies paired-pulse facilitation in area CA1 of the rat hippocampus. *J. Neurophysiol.*, **66**, 1704–1715.

Nitsch, R., Soriano, E. and Frotscher, M. (1990) The parvalbumin-containing nonpyramidal neurons in the rat hippocampus. *Anat. Embryol.*, **181**, 413–425.

Nusser, Z., Roberts, J. D. B., Baude, A., Richards, J. G., Sieghart, W. and Somogyi, P. (1995) Immunocytochemical localization of the α1 and β2/3 subunits of the $GABA_A$ receptor in relation to specific GABAergic synapses in the hippocampal dentate gyrus. *Eur. J. Neurosci.*, **7**, 630–646.

Otis, T. S., de Koninck, Y. and Mody, I. (1993) Characterization of synaptically elicited $GABA_B$ responses using patch-clamp recordings in rat hippocampal slices. *J. Physiol. (Lond.)*, **463**, 391–407.

Otis, T. S. and Mody, I. (1992) Differential activation of $GABA_A$ and $GABA_B$ receptors by spontaneously released transmitter. *J. Neurophysiol.*, **67**, 227–235.

Ramon y Cajal, S. (1893) Estructura del asta de ammon. *Anal. Socied. Hist. Natural.*, **XXII**.

Redman, S. (1990) Quantal analysis of synaptic potentials in neurons of the central nervous system. *Physiol. Rev.*, **70**, 165–198.

Ropert, N., Miles, R. and Korn, H. (1990) Characteristics of miniature inhibitory postsynaptic currents in CA1 pyramidal neurons of rat hippocampus. *J. Physiol. (Lond.)*, **428**, 707–722.

Scharfman, H. E., Kunkel, D. D. and Schwartzkroin, P. A. (1990) Synaptic connections of dentate granule cells and hilar neurons: results of paired intracellular recordings and intracellular horseradish peroxidase injections. *Neuroscience*, **37**, 693–707.

Segal, M. (1990) A subset of local interneurons generate slow inhibitory postsynaptic potentials in hippocampal neurons. *Brain Res.*, **511**, 163–164.

Sloviter, R. S. and Nilaver, G. (1987) Immunocytochemical localization of GABA-cholecystokinin, vasoactive intestinal polypeptide-, and somatostatin-like immunoreactivity in the area dentata and hippocampus of the rat. *J. Comp. Neurol.*, **256**, 42–60.

Solis, J. M. and Nicoll, R. A. (1992) Postsynaptic action of endogenous GABA released by nipecotic acid in the hippocampus. *Neurosci. Lett.*, **147**, 16–20.

Soltesz, I. and Crunelli, V. (1992) A role for low-frequency, rhythmic synaptic potentials in the synchronization of cat thalamocortical cells. *J. Physiol. (Lond.)*, **457**, 257–276.

Soltesz, I. and Deschenes, M. (1993) Low- and high-frequency membrane potential oscillations during theta activity in CA1 and CA3 pyramidal neurons of the rat hippocampus under ketamine-xylazine anesthesia. *J. Neurophysiol.*, **70**, 97–116.

Somogyi, P. and Takagi, H. (1982) A note on the use of picric acid–paraformaldehyde–glutaraldehyde fixative for correlated light and electron microscopic immunocytochemistry. *Neuroscience*, **7**, 1779–1783.

Somogyi, P., Freund, T. F., Hodgson, A. J., Somogyi, J., Beroukas, D. and Chubb, I. W. (1985) Identified axo-axonic cells are immunoreactive for GABA in the hippocampus and visual cortex of the cat. *Brain Res.*, **332**, 143–149.

Somogyi, P., Hodgson, A. J., Smith, A. D., Nunzi, M. G., Gorio, A. and Wu,

J.-Y. (1984) Different populations of GABAergic neurons in the visual cortex and hippocampus of cat contain somatostatin- or cholecystokinin-immunoreactive material. *J. Neurosci.*, **4**, 2590–2603.

Somogyi, P., Nunzi, M. G., Gorio, A. and Smith, A. D. (1983) A new type of specific interneuron in the monkey hippocampus forming synapses exclusively with the axon initial segments of pyramidal cells. *Brain Res.*, **259**, 137–142.

Soriano, E. and Frotscher, M. (1989) A GABAergic axo-axonic cell in the fascia dentata controls the main excitatory hippocampal pathway. *Brain Res.*, **503**, 170–174.

Soriano, E., Nitsch, R. and Frotscher, M. (1990) Axo-axonic chandelier cells in the rat fascia dentata: Golgi—electron microscopy and immunocytochemical studies. *J. Comp. Neurol.*, **293**, 1–25.

Spencer, W. A. and Kandel, E. R. (1961) Hippocampal neuron responses to selective activation of recurrent collaterals of hippocampofugal axons. *Exp. Neurol.*, **4**, 149–161.

Stafstrom, C. E., Schwindt, P. C., Chubb, M. C. and Crill, W. E. (1985) Properties of persistent sodium conductance and calcium conductance of layer V neurons from cat sensorimotor cortex *in vitro*. *J. Neurophysiol.*, **53**, 153–170.

Thompson, S. M. (1994) Modulation of inhibitory synaptic transmission in the hippocampus. *Prog. Neurobiol.*, **42**, 575–609.

Thompson, S. M. and Gahwiler, B. H. (1989) Activity-dependent disinhibition. I. Repetitive stimulation reduces IPSP driving force and conductance in the hippocampus *in vitro*. *J. Neurophysiol.*, **61**, 501–511.

Williams, S. and Lacaille, J.-C. (1992) $GABA_B$ receptor-mediated inhibitory postsynaptic potentials evoked by electrical stimulation and by glutamate stimulation of interneurons in stratum-lacunosum-moleculare in hippocampal CA1 pyramidal cells *in vitro*. *Synapse*, **11**, 249–258.

Ylinen, A., Soltesz, I., Bragin, A., Penttonen, M., Sik, A. and Buzsaki, G. (1995) Intracellular correlates of hippocampal theta rhythm in identified pyramidal cells, granule cells, and basket cells. *Hippocampus*, **5**, 78–90.